Articles

Low-Temperature Hydrothermal Synthesis of Mn_3O_4 and MnOOH Single Crystals: Determinant Influence of Oxidants

Chi-Chang Hu,*,† Yung-Tai Wu,‡ and Kuo-Hsin Chang†,‡

Laboratory of Electrochemistry and Advanced Materials, Department of Chemical Engineering, National Tsing Hua University, 101 Section 2, Kwang Fu Road, Hsin-Chu 30013, Taiwan and Department of Chemical Engineering, National Chung Cheng University, 168 University Road, Min-Hsiung, Chia-Yi 621, Taiwan

Received November 14, 2007. Revised Manuscript Received March 2, 2008

The determinant influences of oxidants on the single-crystalline nature of manganese oxides (i.e., Mn_3O_4 and MnOOH single crystals) through a low-temperature hydrothermal synthesis route from a simple aqueous solution containing 20 mM $Mn(CH_3COO)_2 \cdot 4H_2O$ at 120 °C are demonstrated in this work. The absence of oxygen molecules in the precursor solution limits formation of Mn^{3+}, while saturation of oxygen in the precursor solution causes partial oxidation of Mn^{2+}, favoring direct synthesis of Mn_3O_4 single crystals (hausmannite). Addition of $K_2S_2O_8$ causes complete oxidation of Mn^{2+} to Mn^{3+}, favoring formation of MnOOH single crystals. The shape of as-prepared Mn_3O_4 examined by HR-TEM is polyhedral, i.e., cubic and rhombohedral, while MnOOH prefers to form nanowires. X-ray diffraction, HRTEM, electron diffraction, and Raman spectroscopic analyses confirm the single-crystalline nature of the as-synthesized Mn_3O_4 and MnOOH. With potentiodynamic (CV) activation for 200 cycles between 0 and 1.0 V in 1 M Na_2SO_4 at 25 mV s^{-1}, the activated Mn_3O_4 shows relatively high capacitance (~170 F g^{-1} obtained at 500 mV s^{-1}), high-power nature, and excellent stability for the supercapacitor application. The ideal capacitive responses of activated Mn_3O_4 are definitely different from those of the potentiodynamically activated MnOOH.

Introduction

Manganese oxides of various oxidation states and/or different structures have been attracting considerable research interest due to their promising application potentials in several fields, e.g., catalysis,[1,2] ion exchange,[3,4] molecular adsorption,[5,6] magnetic applications,[7,8] secondary batteries,[9,10] and supercapacitors.[11–13] For instance, Mn_3O_4 has been used as an active catalyst for decomposition of NO_x produced from internal engines and oxidation of benzene or carbon monoxide.[1,2,14] In addition, this oxide was reported to be a promising material in electrochromic applications.[15] On the other hand, MnO_x is widely reported to be a promising electrode material in both alkaline batteries and electrochemical supercapacitors,[11–13,16] which undergoes redox transitions between different oxidation states to store and deliver electric energy. Moreover, MnO_2 exists in many polymorphic forms (such as α, β, γ, and δ), which are different in the linkage of the basic octahedral unit [MnO_6]. They generally show different physicochemical properties for various applications. Furthermore, manganese oxyhydroxide, MnOOH, was used as an effective precursor to synthesize intercalation compounds and lithium manganese oxides for rechargeable lithium-ion batteries.[9] All of the above reports reveal the great interest in synthesizing manganese oxides in various forms/structures for a very wide variety of applications.

* To whom correspondence should be addressed. E-mail: cchu@che.nthu.edu.tw.
† National Tsing Hua University.
‡ National Chung Cheng University.

(1) Yamashita, T.; Vannice, A. *J. Catal.* **1996**, *161*, 254.
(2) Einaga, H.; Futamura, S. *J. Catal.* **2004**, *227*, 304.
(3) Giraldo, O.; Brock, S. L.; Willis, W. S.; Marquez, M.; Suib, S. L.; Ching, S. *J. Am. Chem. Soc.* **2000**, *122*, 9330.
(4) Brock, S. L.; Sanabria, M.; Nair, J.; Suib, S. L.; Ressler, T. *J. Phys. Chem. B* **2001**, *105*, 5404.
(5) Shen, Y. F.; Zerger, R. P.; Deguzman, R. N.; Suib, S. L.; Mccurdy, L.; Potter, D. I.; Oyoung, C. L. *Science* **1993**, *206*, 511.
(6) Lvov, Y.; Munge, B.; Giraldo, O.; Ichinose, I.; Suib, S. L.; Rusling, J. F. *Langmuir* **2000**, *16*, 8850.
(7) Seo, W. S.; Jo, H. H.; Lee, K.; Kim, B.; Oh, S. J.; Park, J. T. *Angew. Chem., Int. Ed.* **2004**, *43*, 1115.
(8) Na, C. W.; Han, D. S.; Kim, D. S.; Park, J.; Jeon, Y. T.; Lee, G.; Jung, M. H. *Appl. Phys. Lett.* **2005**, *87*, 142504.
(9) Thackery, M. M.; Dekock, A.; Rossouw, M. H.; Liles, D.; Bittihn, R.; Hoge, D. *J. Electrochem. Soc.* **1992**, *139*, 363.
(10) Park, K. S.; Cho, M. H.; Park, S. H.; Nahm, K. S.; Sun, Y. K.; Lee, Y. S.; Yoshio, M. *Electrochim. Acta* **2002**, *47*, 2937.
(11) Hu, C. C.; Tsou, T. W. *Electrochem. Commun.* **2002**, *4*, 105.
(12) Junhua, J.; Anthony, K. *Electrochim. Acta* **2002**, *47*, 2381.
(13) Toupin, M.; Brousse, T.; Belanger, D. *Chem. Mater.* **2004**, *16*, 3184.
(14) Johns, M.; Landon, P.; Alderson, T.; Hutchings, G. J. *Chem. Commun.* **2001**, 2454.
(15) Sakai, N.; Ebina, Y.; Takada, K.; Sasaki, T. *J. Electrochem. Soc.* **2005**, *152*, E384.
(16) Im, D.; Manthiram, A. *J. Electrochem. Soc.* **2003**, *150*, A68.

10.1021/cm703245k CCC: $40.75
Published on Web 04/16/2008

On the basis of the above application potentials, there are many studies trying to develop various methods to synthesize manganese oxides of desired forms/structures in order to obtain ideal functions in their unique applications, e.g., calcinations of MnO_2 and Mn_2O_3, surfactant-assisted or ultrasonic-assisted hydrothermal synthesis, chemical bath deposition, sol–gel synthesis, coprecipitation, electrochemical deposition, etc.[11,13,17–24] Very recently, amorphous manganese oxide (denoted as a-MnO_x) prepared by both coprecipitation and electrochemical deposition was found to exhibit ideal capacitive behavior in neutral, aqueous electrolytes. This important finding has attracted more interest in both the synthesis and characterization of various manganese oxides for this high-power application. However, contractions in both electrochemical and textural properties are commonly found. For example, a-MnO_2 prepared by chemical coprecipitation was first announced as an ideal electrode material for the supercapacitor application, while its capacitive performance cannot be obtained if the electronic conductivity of the resultant electrode matrix is not suitably promoted (e.g., by adding 20% carbon).[25] On the other hand, nonstoichiometric a-MnO_x prepared by anodic and potentiodynamic deposition was clearly demonstrated to be responsible for these excellent capacitive properties.[11,26] The charge storage process of a-MnO_2 was reported to follow a very similar mechanism of hydrous RuO_2 (i.e., the double injection/expel of protons and electrons.[27] More recently, the redox transition of manganese oxides was found to involve the exchange of cations (M^+) and electrons, and crystalline M_xMnO_2 was shown to be the main electroactive species for the charge storage/delivery.[13,28]

On the basis of the above viewpoints and facts, a low-temperature (120 °C) hydrothermal synthesis technique is developed to synthesize Mn_3O_4 and MnOOH single crystals from a simple aqueous solution containing 20 mM $Mn(CH_3COO)_2 \cdot 4H_2O$. This work focuses on the determinant influences of oxidants on the crystalline structure of manganese oxides, which are very important in their applications. Furthermore, success in preparing Mn_3O_4 and MnOOH single crystals provides the opportunity to clarify the supercapacitive behavior of electrochemically activated Mn_3O_4 and MnOOH single crystals in aqueous electrolytes because a mixture consisting of Mn_3O_4 nanoparticulates and MnOOH single-crystalline nanowires prepared by means of the sol–gel route was effectively activated by the potentiodynamic route for application of supercapacitors.[19]

Experimental Section

Synthesis of Mn_3O_4 and MnOOH Single Crystals. Mn_3O_4 and MnOOH single crystals were synthesized by means of a simple, low-temperature, hydrothermal method from a 250 mL precursor solution containing 20 mM $Mn(CH_3COO)_2 \cdot 4H_2O$ in a 500 mL Pyrex bottle. Before the hydrothermal step, the precursor solution was saturated with oxygen through pure oxygen bubbling or added with 10 mM $K_2S_2O_8$ in the bottle which was sealed and heated at 120 °C for 12 h. The color of this precursor solution gradually changes from transparent to brown during the heating process, and then, precipitates are clearly found in the bottle. The product, efficiently obtained by means of a centrifuge, was washed with pure water several times until the pH was close to 7. The precipitates were dried in a reduced pressure oven at room temperature overnight (>8 h) for material analysis. For preparation of oxide-coated electrodes, some samples were homogeneously dispersed in pure water to form the coating solution.

Electrode Preparation. The pretreatment procedure of the 10 × 10 × 3 mm graphite supports (Nippon Carbon EG-NPL, N.C.K.) completely followed our previous work.[19] These substrates were drop coated with the well-dispersed as-prepared Mn_3O_4 and MnOOH solutions and further dried in a reduced pressure oven for 8 h at room temperature. All electrodes with an oxide loading of 0.25 ± 0.01 mg cm^{-2} were coated with PTFE films and had an exposed surface area of 1 cm^2 for electrochemical characterization.

Materials Characterization. The nanostructure of Mn_3O_4 and MnOOH single crystals was observed through a transmission electron microscope (FEI E.O Tecnai F20 G2). The surface morphologies were examined by a field-emission scanning electron microscope (FE-SEM, Hitachi S4800-type I). X-ray diffraction (XRD) patterns were obtained with an X-ray diffractometer (Rigaku Miniflex system) using a Cu target (Cu Kα = 1.5418 Å) at an angular speed of 1° (2θ) min^{-1}. The chemical structures of as-prepared manganese oxides were examined by means of a 3D Nanometer Scale Raman PL Microspectrometer (Tokyo Instruments, Inc.) with 632.8 nm radiation from a HeNe laser, which was focused in a circle area less than 1 μm in diameter.

Electrochemical Measurements. Electrochemical characteristics of oxide-coated electrodes were examined by means of an electrochemical analyzer system, CHI 633A (CH Instruments), at 25 °C in a three-compartment cell. An Ag/AgCl electrode (Argenthal, 3 M KCl, 0.207 V vs SHE at 25 °C) was used as the reference, and a piece of platinum gauze was employed as the counter electrode. A Luggin capillary was used to minimize errors due to *iR* drop in the electrolytes. All solutions used in this work were prepared with 18 MΩ cm water produced by a reagent water system (Milli-Q SP, Japan). The electrolytes used for electrochemical characterization were degassed with purified nitrogen gas before measurements for 25 min, and this nitrogen was passed over the solutions during the measurements.

Results and Discussion

Chemistry of the Precursor Solutions. The open-circuit potential−time curves were measured from the precursor solutions with/without addition of oxidants. Typical results measured in a 20 mM $Mn(CH_3COO)_2 \cdot 4H_2O$ solution purged with purified N_2, saturated with purified oxygen, and with addition of 10 mM $K_2S_2O_8$ are shown in Figure 1 as curves 1, 2, and 3, respectively. From curve 1, the open-circuit

(17) Ahmad, T.; Ramanujachary, K. V.; Lofland, S. E.; Ganguli, A. K. *J. Mater. Chem.* **2004**, *14*, 3406.
(18) Xu, H. Y.; Xu, S. L.; Li, X. D.; Wang, H.; Yan, H. *Appl. Surf. Sci.* **2006**, *252*, 4091.
(19) Wu, Y. T.; Hu, C. C. *Electrochem. Solid State Lett.* **2005**, *8*, A240.
(20) Ding, Y. S.; Shen, X. F.; Gomez, S.; Luo, H.; Aindow, M.; Suib, S. L. *Adv. Funct. Mater.* **2006**, *16*, 549.
(21) Yang, X. J.; Tang, W. P.; Feng, Q.; Ooi, K. *Cryst. Growth Des.* **2003**, *3*, 409.
(22) Ferreira, O. P.; Otubo, L.; Romano, R.; Alves, O. L. *Cryst. Growth Des.* **2006**, *6*, 601.
(23) Lei, S. J.; Tang, K. B.; Fang, Z.; Zheng, H. G. *Cryst. Growth Des.* **2006**, *6*, 1757.
(24) Kuratani, K.; Tatsumi, K.; Kuriyama, N. *Cryst. Growth Des.* **2007**, *7*, 1375.
(25) Lee, H. Y.; Kim, S. W.; Lee, H. Y. *Electrochem. Solid State Lett.* **2001**, *4*, A19.
(26) Hu, C. C.; Wang, C. C. *J. Electrochem. Soc.* **2003**, *150*, A1079.
(27) Hu, C. C.; Chen, W. C.; Chang, K. H. *J. Electrochem. Soc.* **2004**, *151*, A281.
(28) Kuo, S. L.; Wu, N. L. *J. Electrochem. Soc.* **2006**, *153*, A1317.

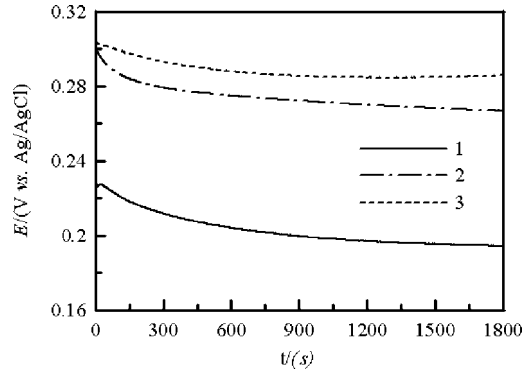

Figure 1. Open-circuit potential against time curves of a 20 mM $Mn(CH_3COO)_2 \cdot 4H_2O$ solution purged with purified (1) N_2 and (2) oxygen and (3) with addition of 10 mM $K_2S_2O_8$.

potential gradually decreases from 0.228 to 0.195 V with prolonging the purging time of purified nitrogen, suggesting continuous removal of dissolved oxygen molecules from the precursor solutions. Curve 2 represents the open-circuit potential of oxygen reduction in the precursor solution since the reaction rate between Mn^{2+} and oxygen molecules is very slow at relatively low temperatures (e.g., 25 °C in this case). This reaction can be accelerated at elevated temperatures since the color of this precursor solution gradually changes from transparent to brown during the heating process, which should obey the following equation

$$4Mn^{2+} + 2H_2O + O_2 \rightarrow 4Mn^{3+} + 4OH^- \qquad (1)$$

However, due to the limited supply and low oxidative ability of oxygen molecules in the precursor solution, the coexistence of Mn^{2+} and Mn^{3+} under the hydrothermal environment favors formation of single-crystalline hausmannite (Mn_3O_4). From a comparison of curves 2 and 3, $K_2S_2O_8$ is clearly demonstrated as a stronger oxidant for oxidation of Mn^{2+}, although the reaction rate between Mn^{2+} and $K_2S_2O_8$ is also slow at low relatively temperatures (e.g., room temperature). Similarly, this reaction is also accelerated during the hydrothermal synthesis period, and addition of $K_2S_2O_8$, causing complete oxidation of Mn^{2+} to Mn^{3+}, favors formation of MnOOH single crystals. This idea is supported by the results that Mn^{2+} will be completely oxidized to Mn^{3+} or Mn^{4+} resulting in formation of MnOOH or MnO_2 crystals by adding various amounts of $KMnO_4$ in Mn^{2+} solutions.[29,30] On the basis of the above results and discussion, we demonstrate a novel idea that the resultant structures of Mn oxides can be effectively controlled by varying the type of oxidants in a hydrothermal synthesis route.

Textural Characterization of Mn_3O_4 and MnOOH Single Crystals. The microstructure of as-prepared Mn_3O_4 and MnOOH are characterized by means of the X-ray diffraction patterns (Figure 2) and Raman spectroscopic analysis (Figure 3). On the basis of pattern 1 in Figure 2, all diffraction peaks can be indexed to the tetragonal hausmannite structure (space group $I41/amd$) of Mn_3O_4 with lattice constants $a = b = 5.762$ Å and $c = 9.470$ Å (JCPDS 24-0734), which are consistent with the standard values of bulk Mn_3O_4. In addition, there are no diffraction peaks corresponding to impurities, suggesting its excellent crystalline quality. This statement is supported by the Raman spectrum shown as curve 1 in Figure 3, which can be used to identify the microstructure information on the molecular scale of as-prepared Mn_3O_4.[18,31] From this Raman spectrum, three main Raman peaks corresponding to crystalline hausmannite structure are clearly found. In addition, there is no red shift for these peaks in comparison with the Mn_3O_4 single crystal, suggesting formation of single-crystalline hausmannite. From pattern 2 in Figure 2, all diffraction peaks correspond to the monoclinic MnOOH [space group $P21/c14$ with lattice constants $a = 5.3$ Å, $b = 5.278$ Å, and $c = 5.307$ Å (JCPDS 41-1379). In addition, the Raman spectrum shown as curve 2 in Figure 3 also indicates the monoclinic MnOOH structure. The above results reveal the fact that the crystalline nature of resultant oxides is determined by the type of oxidants added into the precursor solution. In addition, this work

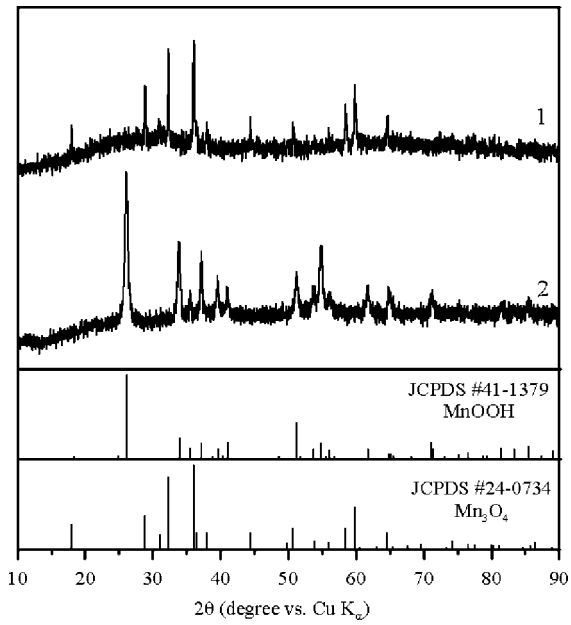

Figure 2. XRD patterns of as-prepared (1) Mn_3O_4 and (2) MnOOH.

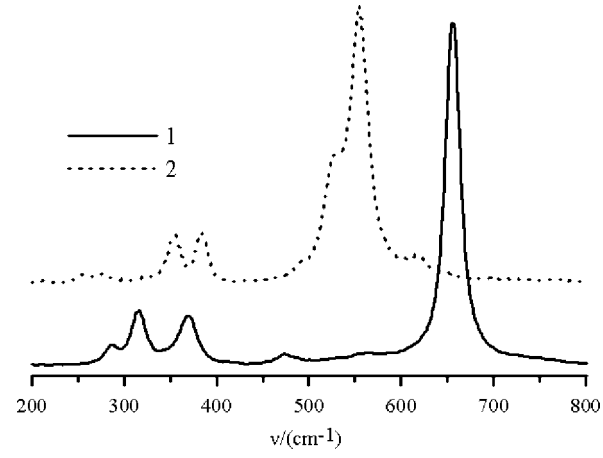

Figure 3. Raman spectra of as-prepared (1) Mn_3O_4 and (2) MnOOH.

(29) Sampanthar, J. T.; Dou, J.; Joo, G. G.; Widjaja, E.; Eunice, L. Q. H. *Nanotechology* **2007**, *18*, 025601.
(30) Crisostomo, V. M. B.; Ngala, J. K.; Alia, S.; Dobley, A.; Morein, C.; Chen, C. H.; Shen, X.; Suib, S. L. *Chem. Mater.* **2007**, *19*, 1832.
(31) Buciuman, F.; Patcas, F.; Craciun, R.; Zahn, D. R. T. *Phys. Chem. Chem. Phys.* **1999**, *1*, 185.

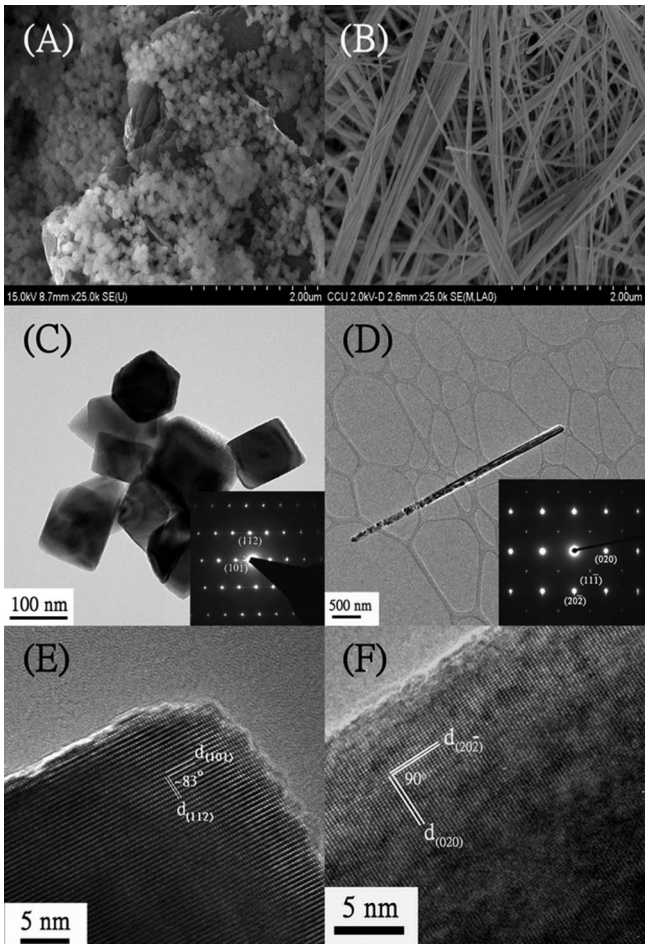

Figure 4. (A,B) FE-SEM and (C−F) HR-TEM images of as-prepared (A,C,E) Mn_3O_4 and (B,D,E) MnOOH; (insets) corresponding SAED patterns.

demonstrates success in synthesizing hausmannite and MnOOH single crystals through a simple, low-temperature, hydrothermal synthesis route.

Note the large quantity of highly pure MnOOH and Mn_3O_4 single crystals in Figure 4A and 4B, further demonstrating success in synthesizing highly pure MnOOH and Mn_3O_4 single crystals via a simple, low-temperature process. The HRTEM and electron diffraction pattern (see Figure 4C) demonstrates the single-crystalline nature of MnOOH. The direction of the zone of electron beam, $[\bar{1}0\bar{1}]$ can be clearly defined from the direction of (020) and $(20\bar{2})$ diffraction dots. The HRTEM image displays the distinct lattice spacing of 2.6 and 2.2 Å, corresponding to the distance of (020) and $(20\bar{2})$ faces, respectively. The HRTEM and electron diffraction pattern (see Figure 4D) demonstrates the single-crystalline structure of Mn_3O_4. The direction of the electron zone, $[\bar{1}3\bar{1}]$, can be clearly defined from the direction of the (112) and $(10\bar{1})$ diffraction dots. The HRTEM image displays a distinct lattice spacing of 4.9 and 3.1 Å, corresponding to a distance of (101) and (112) faces, respectively.

Due to the considerations that the microstructure and electrochemical nature of the electrochemically activated Mn oxide are likely influenced by the original structure of the as-prepared oxides, both Mn_3O_4 and MnOOH single crystals were subjected to electrochemical activation by

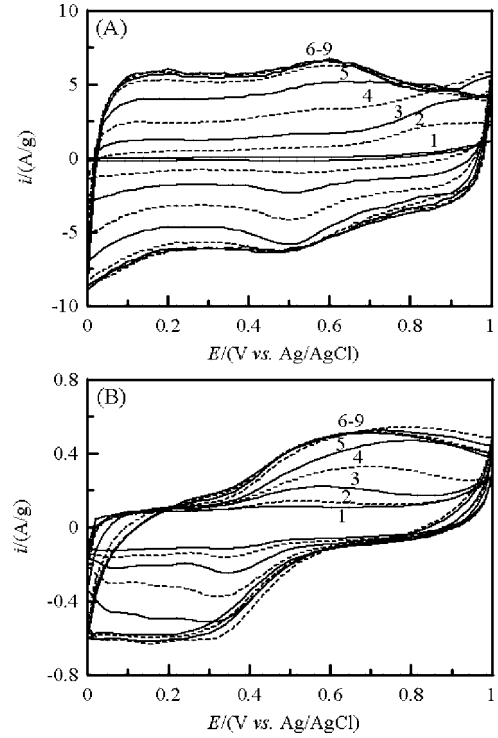

Figure 5. Cyclic voltammograms of (A) Mn_3O_4 and (B) MnOOH with continuous cycling between 0 and 1.0 V for 1500 cycles in 1 M Na_2SO_4 at 25 mV s^{-1}.

repeated potential cycling in order to clarify their electrochemical properties, which are very important in gaining further understanding on the charge storage/delivery mechanism of hydrous Mn oxides. Note in Figure 5A that the pseudocapacitive current density is gradually increased with the number of potential cycling when the cycle number is below 200, which reaches a constant value as the cycle numbers are above 200 (in a 1500-cycle test). The former result indicates that Mn_3O_4 can be easily activated by potential cycling in 1 M Na_2SO_4 between 0 and 1.0 V. The latter result demonstrates the excellent charge/discharge stability of the resultant Mn oxide electrochemically derived from Mn_3O_4. Due to the poor cycling stability of various Mn oxides in neutral media,[26] this merit is believed to be a breakthrough for practical use of manganese oxides in the supercapacitors. Furthermore, activated Mn_3O_4 shows relatively high capacitance ($\sim$170 F g^{-1}) when the scan rate is as high as 500 mV s^{-1}, demonstrating the high-power property. On the other hand, in Figure 5B the pseudocapacitive current density is slowly increased with the number of potential cycling and the voltammetric behavior is poor in the capacitive responses. These results indicate that MnOOH does not exhibit significant redox transitions in the potential region of investigation. This finding is very important because several articles proposed the following mechanism of charge storage/delivery for hydrous MnO_2 in the aqueous, neutral electrolytes[32]

$$MnO_2 + H^+ + e \leftrightarrow MnOOH \qquad (2)$$

However, based on the poor capacitive responses in Figure 5B, MnOOH cannot provide significant pseudocapacitance in the potential region of investigation. Accordingly, MnOOH

is not considered as the electroactive material responsible for the ideal pseudocapacitive behavior of hydrous Mn oxides in neutral media, further clarifying its charge storage/delivery nature. On the other hand, it should be mentioned here that the capacitive properties of Mn oxides may be sensitive to the morphologies, crystal structures, cation valences, and defect chemistry.[26,33,34] The relatively inactive property of MnOOH may be due to the presence of cation valences or the defect chemistry, although MnOOH synthesized in this work has been demonstrated to be single crystalline. Accordingly, the textural information of the Mn oxides after electrochemical activation and effects of cation valences/defect chemistry in the single-crystalline MnOOH and Mn_3O_4 on their electrochemical properties will be investigated in future studies.

(32) Pang, S. C.; Anderson, M. A.; Chapman, T. W. *J. Electrochem. Soc.* **2000**, *147*, 444.
(33) Wei, W.; Chen, W.; Ivey, D. G. *Chem. Mater.* **2008**, . (ASAP article).
(34) Wei, W.; Chen, W.; Ivey, D. G. *J. Phys. Chem. C* **2007**, *111*, 10398.

Conclusions

Single-crystalline Mn_3O_4 and MnOOH were successfully synthesized using a simple, low-temperature, hydrothermal process. The single-crystalline nature of resultant manganese oxides is determined by the type of oxidants added into the precursor solution. The ideal capacitive responses of electrochemically activated Mn_3O_4 are definitely different from the poor capacitive behavior of the potentiodynamically activated MnOOH, revealing that MnOOH is not the electroactive material responsible for the pseudocapacitive reactions of hydrous Mn oxides in neutral media, although the capacitive properties of Mn oxides may be sensitive to their morphologies, crystalline structures, cation valences, and defect chemistry.

Acknowledgment. The financial support of this work, by the National Science Council of ROC, under contract no. NSC 96-2214-E-194-001, is gratefully acknowledged.

CM703245K